Performance Analysis of ASR-UKFs for Supercapacitor SoC Estimation in Hybrid Energy Storage Systems

Davide Fusco, Seyede Masoome Maroufi, *Student Member, IEEE,* Francesco Porpora, *Member, IEEE,* Mauro Di Monaco, *Member, IEEE,* Giovanni De Carne, *Senior Member, IEEE,* Giuseppe Tomasso, *Member, IEEE*

***Abstract*—Due to their high specific power and durability, supercapacitors are promising candidates to be formed with batteries in Hybrid Energy Storage Systems (HESS). Accurately determining the supercapacitor's State of Charge (SoC) represents a crucial task and improves system performance and energy management. In this paper, state-of-the-art algorithms to assess the SoC of supercapacitors are initially described, and their performances have been compared in simulation and validated experimentally. To improve the estimation performance, an Adaptive Square-Root Unscented Kalman Filter method has been finally proposed in this paper. Two electric circuit models have been defined for implementing the Kalman filtering method and analyzing its performance. Numerical results demonstrated a 7% estimation error reduction in terms of absolute value with respect to the conventional methods. Moreover, an estimation error lower than 1.5% has been achieved by the proposed method in experimental tests under realistic grid power profile, validating the numerical results and demonstrating the applicability of the developed estimator for supercapacitor SoC estimation.**

***Index Terms*—Energy Storage, Hybrid energy storage, Kalman Filter, Parameter estimation, State of Charge, Supercapacitor.**

I. Introduction

One of the leading solutions to address the challenge of global warming through integrating Renewable Energy Sources (RES) in the power system is using Energy Storage Systems (ESS). With the deployment of ESS in an electricity system, voltage instability, frequency fluctuation, poor power quality, load-following, and other power system challenges could be mitigated [1]–[3].

Among the most promising ESSs, electrochemical ones such as secondary metal-ion batteries and supercapacitors can be distinguished for their high efficiency, flexibility, and versatility [4]. Despite batteries can be developed for high-power and/or energy density, they still have a lower power capability for fast charging/discharging with respect to supercapacitors [5]. Therefore, in order to achieve high power and energy density at the same time, a hybrid system consisting of two ESS can be introduced [6]–[8]. Hybrid Energy Storage System (HESS) solves the problems faced by the grid integration of alternative single-energy storage systems regarding simultaneously meeting the needs of high specific power and high specific energy. Moreover, it helps to reduce the battery's size and increase its lifespan [9]–[11]. However, the key issues are energy management and power sharing between the two ESS while using them in the hybrid mode [12]. Indeed, high performances in the HESSs control strategies are achieved by considering an effective power allocation strategy during system operation [13]. For this reason, the knowledge of system states is of paramount importance. One of the main challenges is represented by the SoC estimation in energy storage devices such as Supercapacitors [14]–[16] that represents an indication of the actual available energy compared to the maximum energy stored in it. However, commonly adopted methods lack in considering nonlinear behavior and typical leakage effects of supercapacitors, thus leading to consistent inaccuracies in the SoC indication. The more advanced methods in SoC estimation mostly present a model-based approach and the most reliable ones are based on the state observers, such as Kalman Filters (KF), since they are not affected by measurement errors and noise [17], [18]. An Adaptive Square-Root Unscented Kalman Filter (ASR-UKF) is proposed in [19], [20] and its higher performance with respect to other algorithms is proven in the case of battery state of charge estimation [21]. However, the use of the same filter for supercapacitor SoC estimation has not been found in the literature, to the best of the authors' knowledge. Therefore, an investigation on their applicability as well as their performance in supercapacitor state estimation is worth to be performed. Another important aspect to analyze is the choice of a system model, which is crucial for ensuring good performances in model-based state estimation algorithms. Good modeling accuracy and low computational cost for real-time implementation are common requirements and Equivalent Circuit Models (ECMs) are proven to be the best candidates, providing a good trade-off between accuracy and complexity [22]–[24]. A different approach is represented by intelligent modeling techniques, such as data-driven Artificial Neural Networks (ANN) and fuzzy logic, which result in good modeling capability [25]. However, the considerable effort in the training process and the need for large amounts of data to ensure robustness and model accuracy strongly limit their adoption [26].

In this paper, two state estimators, derived by the integration of different models with an ASR-UKF, have been implemented for evaluating the estimation performance in supercapacitors.

The work of Masoome Seyede Maroufi and Giovanni De Carne has been supported by the Helmholtz Association under the program "Energy System Design" and under the Helmholtz Young Investigator Group "Hybrid Networks" (VH-NG-1613).

The estimators are versatile techniques applicable to supercapacitors across various systems, independent of their specific use. Hence, the suggested approach can be applied across diverse systems, considering the effort involved in characterizing and implementing an appropriate model. The focus on HESS applications stems from the fact that supercapacitors are frequently used in this field, particularly in conjunction with high-energy batteries. The estimation performances have been compared to the main conventional methods commonly adopted for evaluating the stored energy in supercapacitors, and the improvements in SoC estimation given by the proposed algorithm are highlighted. In particular, the following novelties are presented with respect to the state of the art.

- An ASR-UKF has been designed for Supercapacitor State of Charge estimation.
- The initialization of the KF has been performed by means of a parameter estimator tool, alternatively to the more common trial and error procedures.
- Two different ECM have been integrated with the ASR-UKF, and their impact on estimation performances has been evaluated.
- The ASR-UKF approach has been validated experimentally under realistic grid power profiles.

Considering the lack of methodologies for supercapacitor state estimation based on the ASR-UKF, the proposed method represents a novel approach for the SoC estimation in supercapacitors. Moreover, the performance comparison carried out by considering two different system models strongly contributes to further increase the knowledge about SoC estimation for supercapacitors. The rest of the paper is organized as follows. In section II, the conventional SoC estimation methods and the more advanced SR-UKF, with details of the adaptive algorithm considered for obtaining the proposed ASR-UKF, are introduced. In section III, the two different electric circuit models considered in this work are described. Section IV depicts the numerical results, and section V shows the results obtained in experimental analysis. In addition, the experimental results obtained by emulating realistic grid power scenarios are reported in section VI. Finally, the conclusions are reported in section VII.

II. State of Charge Estimation

In HESS, accurate knowledge of SoC is paramount since it allows for maximizing system performance and improving energy management strategies while ensuring safe operating conditions. Nevertheless, the amount of energy stored in a supercapacitor is not directly measurable, and internal nonlinear phenomena make the online SoC estimation challenging.

A. Conventional methods

Among the conventional methods, the simple capacitive model considers the supercapacitor as a standard capacitor and defines the SoC as the ratio between the actual stored energy and the maximum available energy [27], [28]. The actual stored energy is derived from the supercapacitor terminal voltage measurement, while the maximum available energy is derived from its capacity and nominal voltage values. This estimation method is identified as the State of Art, and the related SoC calculation results (SoC_{SoA}) are as follows:

$$SoC_{SoA} = \frac{\frac{1}{2}C_n v_{sc}^2}{\frac{1}{2}C_n V_n^2} = \frac{v_{sc}^2}{V_n^2} \tag{1}$$

where v_{sc} is the measured capacitor voltage, and C_n and V_n are the rated capacity and voltage, respectively. This definition is mostly used thanks to its simplicity and easy implementation. However, the supercapacitor non-linear behavior, comprising internal losses and internal charge redistribution effect, is not taken into account in this method, which inevitably leads to consistent errors in SoC tracking. A more accurate indication can be achieved by monitoring the energy accumulated in internal modeled capacitance if a R-C multi-branch model is implemented. In this way, the internal charge redistribution is also taken into consideration [29]. In detail, the SoC given by a multi-branch model, namely SoC_{MB}, results as follows:

$$SoC_{MB} = \frac{\sum_{i=1}^{n} \frac{1}{2}C_i v_i^2}{E_{max}} \tag{2}$$

where n is the number of internal states included in the model, C_i and v_i is the modeled internal capacitance values of the supercapacitor and the voltage across them, respectively, and E_{max} represents the characterized maximum energy considering all the internal states. Alternatively, the Coulomb Counting method is commonly used in real-world applications for online estimation purposes. It relies on the integration of the supercapacitor current over time to the online evaluation of the stored energy. Starting from a known initial state SoC_0, the actual SoC value SoC_{CC} at time t is obtained as follows:

$$SoC_{CC} = SoC_0 - \frac{1}{C_{Ah}} \int_0^t I_{sc}(t)\, dt \tag{3}$$

where C_{Ah} is the rated capacity expressed in ampere-hour, and I_{sc} is the measured current. However, this method is sensitive to measurement error and noise, and estimation performance also relies on the accuracy of the initial estimated SoC value. As a consequence, the estimation performance worsens over time [28]. The accumulated error is usually cleared, assuming a linear relationship between SoC and the Open Circuit Voltage (OCV). OCV is used to interpolate the initial value SoC_0, but it has to be previously determined in offline characterization. The OCV-SoC relation ignores the typical nonlinear behavior of the supercapacitors, such as the voltage-dependent capacity term. Moreover, a minimum rest period with zero current is needed to properly observe the OCV, which is rarely feasible in practical applications.

Above mentioned methods are suitable in many cases when accuracy is not of primary importance and simplicity of implementation is needed. On the other hand, in the HESS application field, estimation accuracy plays an important role in energy management and real-world effects impacting the supercapacitor's available energy. For instance, the internal charge redistribution and leakage effect cannot be neglected. Hence, more advanced and reliable approaches are worth to be considered.

TABLE I
STATE OF THE ART ON SUPERCAPACITOR SOC ESTIMATION METHODS

Reference	Method	Supercap application	Real-Time	Different models comparison	Training data required
[30]	ASR-UKF	✗	✓	✗	✗
[23]	UKF	✓	✗	✗	✗
[31]	ANN	✗	✗	✗	✓
[25]	ANN	✓	✗	✗	✓
[27]	KF	✓	✓	✗	✗
[28]	Luenberger	✓	✓	✗	✗
[32]	KF-PF	✓	✗	✗	✗
[33]	Multi-observer	✓	✗	✗	✗
Proposed method	ASR-UKF	✓	✓	✓	✗

B. Kalman Filtering Method

Kalman Filter (KF) as an optimal state estimator [17] in linear systems was introduced in 1960. During the past years, KFs have been adopted in the implementation of several nonlinear applications. The Extended Kalman Filter (EKF) achieves the integration of a nonlinear model by means of a first-order Taylor-series expansion [18]. An application of the Kalman filtering method for SoC tracking in suppercapacitors, by considering a three-branch model, has been proposed in [27]. The method has been validated over a series of charging/discharging profiles but only the simple capacitive model has been included in the comparison. The Unscented Kalman Filter (UKF) introduces a deterministic sampling approach, increasing robustness to strong nonlinearities in the system [34]. The method has been proposed for supercapacitor SoC estimation by considering a first-order dynamic Equivalent Circuit Model in [23]. The experimental results demonstrated its robustness to parameter variation. However, the estimation performances have not been compared with other methods or supercapacitor models.

The Square-Root Unscented Kalman Filter (SR-UKF) represents a more efficient mathematical implementation, as stated in [35], and its integration with an adaptive algorithm has been proposed in [30]. The higher estimation accuracy compared to the other KFs has been reported [36], but its application to supercapacitor SoC estimation is not documented in the actual literature. The adoption of a fractional order model, leading to a fractional Kalman filtering approach, is discussed in [32]. This model involves identifying a considerable number of parameters, and the combination of the Kalman filter with a particle filter (KF-PF) introduces significant complexity. Although [32] reports good estimation accuracy, the estimation performed on a host PC does not ensure real-time execution, and only a comparison with the Ampere-hour integral method is provided.

Another estimation scheme, based on a multiobserver framework, is presented in [33]. This method achieves accurate and robust SoC estimation but requires additional modeling effort due to the integration of multiple models. Furthermore, the experimental validation was conducted using experimental data in the Matlab/Simulink environment, and real-time execution has not been addressed. A comparison between the proposed estimation method and the main contributions from the state-of-the-art literature is summarized in Table I, highlighting the main benefits and drawbacks of the mentioned estimators.

In this paper, the adaptive algorithm presented in [19], [30] for Lithium-Ion batteries SoC estimation has been implemented for the state estimation of supercapacitors. The considered adaptive law updates the covariance matrices at each iteration step based on the voltage residual covariance, which is calculated to represent the error of the model output estimated by the filter compared to the measured output. The obtained algorithm overcomes the initial parameter tuning issue while improving the estimation performance and robustness under real operating conditions. More details regarding the main operations of the ASR-UKF algorithm for SoC estimation and the related implementation are reported in [19], [35].

C. Kalman Filter Initialization

In Kalman Filtering methods, an initial calibration based on system dynamics has to be made to guarantee the algorithm's best performance and robust operation. In particular, the measurement noise covariance R, the process noise covariance Q, and the initial state covariance S_0, are set as diagonal matrices. This means only the auto-covariance terms are considered, and the involved noise terms are independent. Since these factors influence filter convergence and estimation performance, a charging/discharging current profile can be defined to validate their initialization. Therefore, as part of the modeling procedure, an optimal calibration is achieved by fitting the filter estimated state variables onto the ideally simulated ones by means of the "Parameter Estimator" app tool in Matlab-Simulink®. The toolbox implements the nonlinear least square solver to minimize the error in the chosen model outputs. The obtained parameters represent the optimal choice for the Kalman Filter initialization in the predefined operating conditions.

III. SUPERCAPACITOR MODEL

A proper model of the real system needs to be defined to implement an effective and reliable model-based state estimation

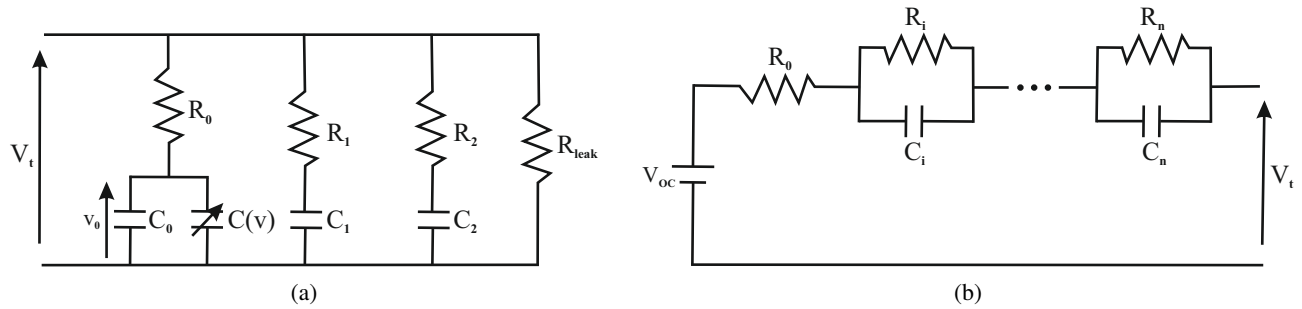

Fig. 1. Supercapacitor equivalent models: (a) Three-Branch Electric Circuit Model and (b) Generic n-Order Dynamic Equivalent Circuit Model.

algorithm, such as the Kalman Filtering method. Mainly, two different Equivalent Circuit Models (ECM), namely the three-branch model and the first-order ECM, can be considered for representing the supercapacitor's behavior. The first one has been proven as the best trade-off between model accuracy and computational cost for real-time implementation [22], [37]. Still, a lack of explicit SoC derivation from the model equations has to be taken into account, which makes its identification not a straightforward task. On the other hand, dynamic ECMs including a direct correlation between the actual SoC state and the modeled Open Circuit Voltage, as well as the additional model parameters, present an easier SoC identification by integrating its computation with the model equations. Despite their lower accuracy in representing the supercapacitor nonlinear behavior with respect to three-branch models, the applicability of first-order dynamic ECMs for supercapacitor SoC estimation has been reported in the literature [23], [24]. However, a comparison between the different modeling techniques and their impact on SoC estimation performances is poorly documented. In this section, the investigation of supercapacitor modeling approaches is reported. The aforementioned ECMs have been considered for representing the supercapacitor's behavior, and their suitability for SoC estimation techniques as well as the related impact on the model-based estimation performance have been analyzed.

A. Three-Branch Equivalent Circuit Model

Fig. 1(a) illustrates the electrical circuit of a three parallel branches dynamic model [38]. It comprises a main RC branch with two parallel-connected RC branches. In the main branch, the basic nonlinear capacitive effect is represented by the capacitor $C(v)$ connected in series with the resistor R. The capacitance dependency on the voltage is taken into account as follows:

$$C(v) = C_0 + K_v \cdot v_0 \tag{4}$$

where C_0 represents the fixed capacitance of the supercapacitor and K_v is the factor describing the dependency of the capacitance on its voltage v_0. The two additional RC branches, namely $R_1 - C_1$ and $R_2 - C_2$, are included in the model for distinguishing two different time constants, accounting for the dynamics related to the ion diffusion effect [38]. A leakage resistor R_{leak} for representing the self-discharge effect is also included, and its value is usually declared on the manufacturer datasheet. According to Kirchhoff laws, system equations can be worked out from the ECM as follows:

$$\begin{cases} C(v_0)\dfrac{dv_0}{dt} = -\dfrac{R_p}{R_0}\left(\dfrac{1}{R_1}+\dfrac{1}{R_2}\right)v_0 + \dfrac{R_p}{R_0R_1}v_1 + \\ \qquad + \dfrac{R_p}{R_0R_2}v_2 + \dfrac{R_p}{R_0}I \\ C_1\dfrac{dv_1}{dt} = \dfrac{R_p}{R_0R_1}v_0 - \dfrac{R_p}{R_1}\left(\dfrac{1}{R_0}+\dfrac{1}{R_2}\right)v_1 + \\ \qquad + \dfrac{R_p}{R_1R_2}v_2 + \dfrac{R_p}{R_1}I \\ C_2\dfrac{dv_2}{dt} = \dfrac{R_p}{R_0R_2}v_0 + \dfrac{R_p}{R_1R_2}v_1 + \\ \qquad - \dfrac{R_p}{R_2}\left(\dfrac{1}{R_1}+\dfrac{1}{R_0}\right)v_2 + \dfrac{R_p}{R_2}I \\ V_t = \dfrac{R_p}{R_0}v_0 + \dfrac{R_p}{R_1}v_1 + \dfrac{R_p}{R_2}v_2 + R_pI \end{cases} \tag{5}$$

where $R_p = R_0 \parallel R_1 \parallel R_2 \parallel R_{leak}$ and v_1 and v_2 are the voltages on capacitors C_1 and C_2, respectively.

Considering $x = [v_0, v_1, v_2]$ the state variables, the discrete-time model equations can be derived as shown in (6) and (7), where T_s is the period of the execution time-step, and k indicates the discrete k-th iteration. As can be noticed, the model is highly effective if the objective is voltage monitoring since the internal voltages of the supercapacitors are the state variables, but in the model, there is not an explicit relation with the SoC. Therefore, the voltages across the three modeled internal capacitors (v_0, v_1, and v_2) have been considered for enabling the SoC computation, according to (2). In addition, considering the minimum operating voltage of a supercapacitor, usually determined as half of the maximum voltage, a relative indication has been adopted according to (8):

$$SoC_{3B} = \frac{\sum_{i=1}^{n}\frac{1}{2}C_i v_i^2 - E_{min}}{E_{max} - E_{min}} \tag{8}$$

where E_{min} is the minimum necessary energy to be stored in the supercapacitor to operate it fully, and it is defined as:

$$E_{min} = \sum_{i=1}^{n}\frac{1}{2}C_i v_{min}^2 \tag{9}$$

B. First-order dynamic Equivalent Circuit Model

Electric circuit models are widely adopted in battery state of art for representing equivalent electrical behavior. The electrical characteristic of a supercapacitor can be considered similar to the battery case if the different voltage range exhibited by the device is taken into account. Therefore, the behavior of a

supercapacitor can be represented by an ideal voltage source (V_{oc}) connected in series with a resistor R_0 and one or more parallel branches R_i-C_i, as illustrated in the model equivalent circuit in Fig. 1(b).

In this paper, a first-order ECM has been considered, since it is proven to provide good modeling accuracy and acceptable complexity in comparison with higher order ECMs. Moreover, considering the typical voltage response of a supercapacitor it results sufficiently accurate for reproducing the modeled electrical behavior [28]. The model includes an Open Circuit Voltage (V_{oc}) representing the SoC-dependent voltage shown by the device in no-load condition, an equivalent series internal resistance R_0 mainly due to non-ideal contacts and electrodes, and a $R_1 - C_1$ branch related to the internal charge redistribution and ion diffusion effect. The selected model allows for representing the main nonlinear supercapacitor behavior and results in a locally observable ECM providing the SoC information as an explicit state variable [23], [39]. Since SoC is a variable in the system, the Coulomb Counting method is included in the model, and the following equations are obtained:

$$\begin{cases} SoC = SoC_0 - \dfrac{1}{3600 \cdot C_{Ah}} \displaystyle\int_0^t I_{sc}\,(t)\,dt \\ \dfrac{dv_1}{dt} = -\dfrac{v_1}{R_1 C_1} + \dfrac{I_{sc}}{C_1} \\ V_t = V_{oc} - R_0 \cdot I_{sc} - v_1 \end{cases} \tag{10}$$

where v_1 is the voltage across the $R_1 - C_1$ branch, and I_{sc} is the current flowing in the supercapacitor, being positive for discharging and negative for the charging phase. The state variables are chosen as $x = [SoC, V_1]$ and the discrete-time model equations are derived as shown in (11) and (12).

$$\begin{bmatrix} SoC_{k+1} \\ V_{1,k+1} \end{bmatrix} = \begin{bmatrix} SoC_k - \dfrac{T_s}{3600 \cdot C_{Ah}} \cdot I_{sc} \\ \left(\dfrac{T_s}{R_1 C_1}\right) \cdot V_{1,k} + \dfrac{T_s}{C_1} \cdot I_{sc} \end{bmatrix} \tag{11}$$

$$V_{t,k} = V_{oc} - R_0 \cdot I_{sc} - V_{1,k} \tag{12}$$

C. Model Parameters Extraction

The models mentioned in section III-A and III-B have been characterized in a laboratory environment testing an EATON 166F supercapacitor (model XLR-48R6167-R) as Device Under Test (DUT). The main characteristics of the device and their nominal values, given by the manufacturer, are reported in table II. Note that, in the three-branch ECM, the parameters are not correlated to the SoC values since they are constant at any SoC condition of the supercapacitor. The capacity variability is expressed by means of the K_v factor, which multiplied by the voltage v_0 represents the capacitance dependency on the voltage, according to (4).

TABLE II
EATON XLR 166F SUPERCAPACITOR SPECIFICATIONS

Parameter	Value
Capacitance (F)	166
Maximum working voltage (V)	48.6
Equivalent Series Resistance (mΩ)	5
Nominal leakage current (mA)	5.2
Stored energy at the maximum voltage (Wh)	54
Nominal continuous current (A)	86
Peak power (kW)	118
Pulse current (A)	2200

A charging/discharging repeating cycle has been experimentally performed by imposing constant current steps on the device to calibrate the three-branch model. In this way, the DUT is charged and discharged four times between a selected minimum voltage level and its nominal value, applying 20 seconds rest period between each phase of the test. The supercapacitor voltage and current measurements during the experimental characterization are illustrated in Fig. 2(a). The extraction of the model parameters has been made by means of the "Parameter Estimator" tool in Matlab-Simulink®. It allows for fitting the model voltage curve to the measured one by selecting the same current input given by the experimental test. As a solver, the nonlinear least square method has been selected, and the obtained parameters are reported in table III.

The second model in the analysis involves SoC-dependent parameters to enable direct observability of the State of Charge as a state variable. Therefore, a specific procedure for characterizing the model parameters is needed. The model is widely adopted for Lithium-Ion batteries, and a well-known characterization procedure is the Hybrid Pulsed Current Characterization (HPPC) [40]. It involves 20 seconds of current pulses executed at incremental SoC values, assuming it to be unaffected by the short duration of the pulses. However, in the case of a supercapacitor, the same assumption is harder to guarantee due to the device's lower capacity. Hence, the similar Positive Pulsed Current (PPC) approach was adopted [41] and shorter current pulses were exploited for increasing the supercapacitor SoC and concurrently identifying the parameters of the equivalent circuit model. The procedure has been performed at different charging/discharging current levels, and Fig. 2(b) shows the current and voltage acquired during a nominal current test as an example. It consists in constant current pulses maintained for the necessary time to

$$\begin{bmatrix} V_{0,k+1} \\ V_{1,k+1} \\ V_{2,k+1} \end{bmatrix} = \begin{bmatrix} \left(1 - \dfrac{R_p T_s}{R_0 C(v)}\left(\dfrac{1}{R_1} + \dfrac{1}{R_2}\right)\right) V_{0,k} + \left(1 + \dfrac{R_p T_s}{R_0 R_1 C(v)}\right) V_{1,k} + \left(1 + \dfrac{R_p T_s}{R_0 R_2 C(v)}\right) V_{2,k} + \dfrac{R_p T_s}{R_0 C(v)} I_k \\ \left(1 + \dfrac{R_p T_s}{R_0 R_1 C_1}\right) V_{0,k} + \left(1 - \dfrac{R_p T_s}{R_1 C_1}\left(\dfrac{1}{R_0} + \dfrac{1}{R_2}\right)\right) V_{1,k} + \left(1 + \dfrac{R_p T_s}{R_1 R_2 C_1}\right) V_{2,k} + \dfrac{R_p T_s}{R_1 C_1} I_k \\ \left(1 + \dfrac{R_p T_s}{R_0 R_2 C_2}\right) V_{0,k} + \left(1 + \dfrac{R_p T_s}{R_1 R_2 C_2}\right) V_{1,k} + \left(1 - \dfrac{R_p T_s}{R_2 C_2}\left(\dfrac{1}{R_1} + \dfrac{1}{R_0}\right)\right) V_{2,k} + \dfrac{R_p T_s}{R_2 C_2} I_k \end{bmatrix} \tag{6}$$

$$V_{t,k} = \frac{R_p}{R_0} v_{0,k} + \frac{R_p}{R_1} v_{1,k} + \frac{R_p}{R_2} v_{2,k} + R_p I_k \tag{7}$$

TABLE III
FITTED PARAMETERS FOR THE THREE-BRANCH SUPERCAPACITOR MODEL

Parameter	C_0 (F)	K_v (F/V)	R_0 $(m\Omega)$	R_1 (Ω)	C_1 (F)	R_2 (Ω)	C_2 (F)	R_{leak} $(k\Omega)$
Value	132.78	1.08	5.2	11.01	6.61	159.96	2.38	9.5

TABLE IV
EXTRACTED PARAMETERS WITH PPC PROCEDURE FOR THE FIRST ORDER ECM

	SoC $(\%)$	V_{oc} (V)	R_0 $(m\Omega)$	R_1 $(m\Omega)$	C_1 (kF)
Discharge	10	6.08	2.7	2.6	4.77
	20	11.28	2.7	2.1	5.47
	30	16.28	2.7	1.9	5.97
	40	21.09	2.7	1.8	5.79
	50	25.73	2.6	1.7	5.65
	60	30.27	2.7	1.6	5.63
	70	34.73	2.8	1.4	5.75
	80	39.14	2.8	1.1	5.52
	90	43.51	2.6	0.8	3.90

	SoC $(\%)$	V_{oc} (V)	R_0 $(m\Omega)$	R_1 $(m\Omega)$	C_1 (kF)
Charge	10	5.98	2.8	1.2	7.55
	20	11.62	2.8	1.6	6.23
	30	16.92	2.7	1.8	5.95
	40	21.92	2.7	2.1	5.64
	50	26.71	2.7	2.5	5.25
	60	31.34	2.7	2.8	4.82
	70	35.85	2.6	3.2	4.42
	80	40.26	2.8	3.3	4.31
	90	47.03	2.6	4.0	3.78

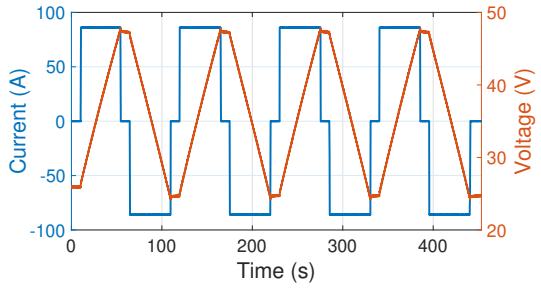

(a)

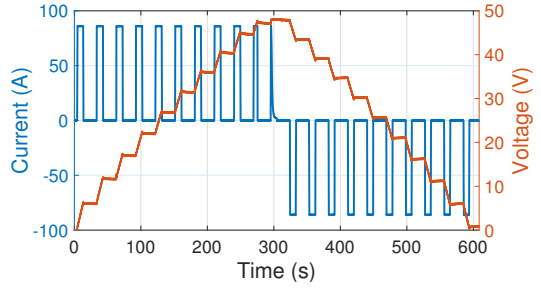

(b)

Fig. 2. Experimental characterization of the supercapacitor: measured current and corresponding terminal voltage during the procedure related to (a) three-branch model and (b) first-order dynamic Equivalent Circuit Model.

charge or discharge the DUT by a 10% SoC value. Between two consecutive pulses, a 20 seconds rest time is observed. The voltage measured during each resting interval is used for parameter estimation, which results related to the SoC value reached during the previous current pulse. In particular, the series resistance R_o is responsible for the voltage drop ΔV occurring at the moment the current is stopped, and it is derived by dividing ΔV by the current pulse amplitude. The second part of the voltage relaxation is modeled by the fitting of an RC exponential voltage response curve, thus obtaining the values of R_1 and C_1. The different procedures for characterizing the two models were executed with a nominal current amplitude of 86 A for charging and discharging the supercapacitor. The model parameters obtained from the PPC characterizing procedure are listed in table IV, distinguished in the charging and discharging phases.

IV. NUMERICAL RESULTS

To compare their performances, all the SoC estimation methods mentioned in the previous section have been implemented in Matlab-Simulink. The three-Branch model and the first-order ECM have been implemented as a plant model for simulating the supercapacitor behavior and random noise has been added to voltage and current measurements for reproducing a realistic acquisition environment. The model equations described in sections III-A and III-B have been included in two different ASR-UKFs for evaluating the impact of the two modeling approaches on the proposed adaptive algorithm. Moreover, all the estimation results have been scaled down to represent the SoC state with respect to the voltage operating range of the supercapacitor, thus obtaining a relative indication for a more practical SoC evidence and an effective comparison between the different methods. Finally, the absolute value of the error with respect to the reference SoC, computed as in (13), has been considered as a performance indicator for each method.

$$\varepsilon = |SoC_{est} - SoC_{ref}| \tag{13}$$

where SoC_{est} is the estimated SoC. Similar to the modeling procedure, a constant current is imposed on the device for pre-charging it to the minimum operating voltage. After a resting time, a sequence of charging and discharging pulse current is adopted for testing the performances of the estimation algorithms. The numerical SoC estimation results obtained from the four SoC computation methods are shown in Fig. 3(a), where the true SoC reference SoC_{ref} has been computed on the basis of the ideal internal supercapacitor voltages. The SoC_{SoA} and the SoC_{CC} are the SoC estimations resulting from the State of the Art and the Coulomb Counting methods, according to (1) and (3), respectively. The SoC estimation results obtained from the proposed adaptive algorithm integrated with the first-order ECM and the three-branch ECM are indicated as ASR-UKF$_{\text{ECM}}$ and ASR-UKF$_{\text{3B}}$, respectively. The estimation errors with respect to the reference SoC are illustrated in Fig. 3(b). The conventional methods and the ASR-UKF integrating the first-order ECM achieved similar estimation performances, reaching a maximum estimation error of above 8% in absolute value. The significant uncertainty of

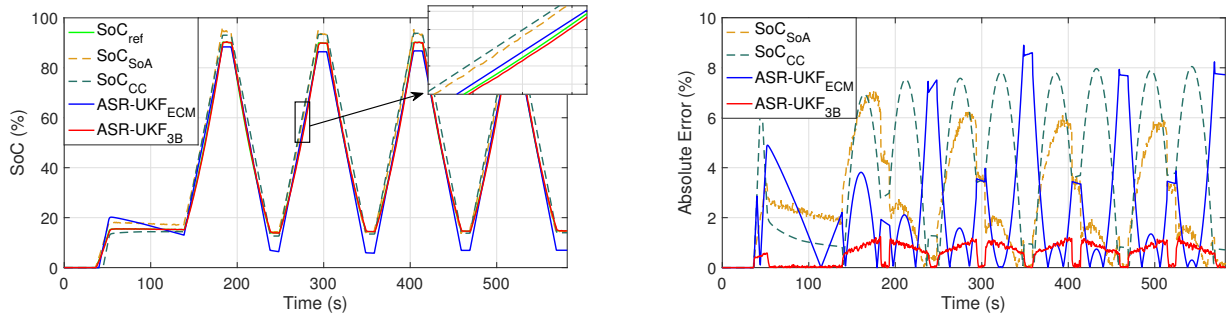

(a) (b)

Fig. 3. Numerical results for SoC estimation: (a) SoC estimation results and (b) errors with respect to the ideal SoC reference.

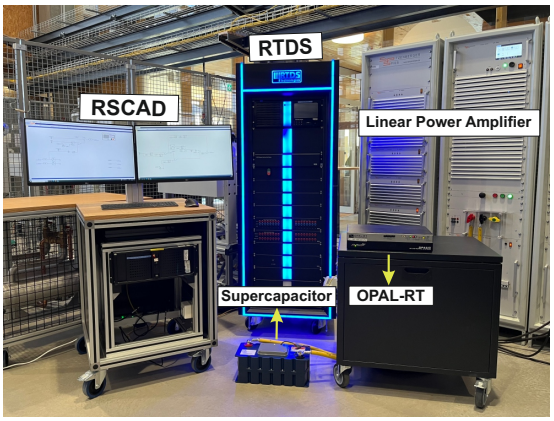

Fig. 4. Experimental setup for the supercapacitor SOC estimation.

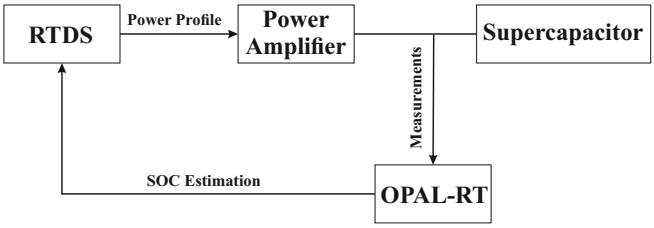

Fig. 5. Supercapacitor SoC estimation hardware diagram.

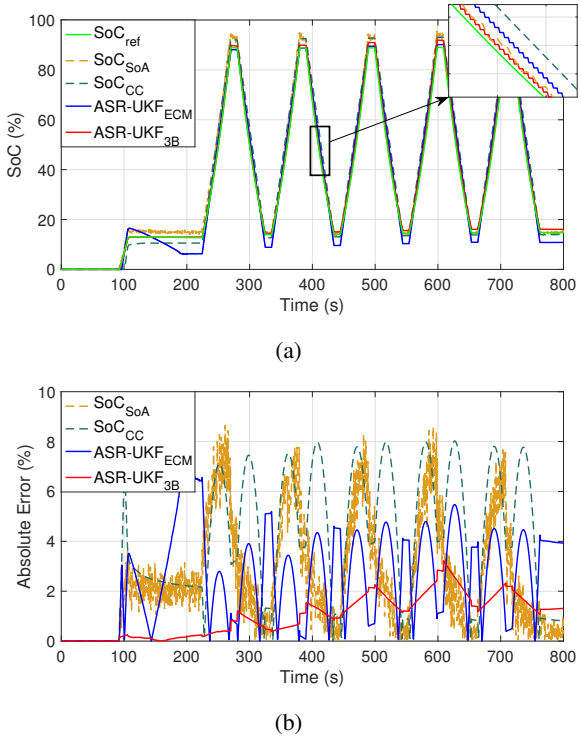

(a) (b)

Fig. 6. Experimental results for real-time SoC estimation: (a) SoC estimation results and (b) errors with respect to the ideal SoC reference.

these methods is mainly due to the smaller device capacity and the higher current rates in faster time periods with respect to a typical battery storage application. In particular, the Coulomb Counting method results in worse estimation performances when applied to supercapacitors, since it does not take into account nonlinear behaviors such as the typical supercapacitor internal voltage redistribution and voltage-dependent capacity. On the other hand, the proposed ASR-UKF guarantees the best estimation performances if the three-branch model is considered for representing the supercapacitor dynamic behavior, in which case an estimation error lower than 1% in absolute value has been achieved during the entire test profile.

V. Experimental Results

An experimental setup has been carried out to validate the numerical results and the proposed SoC estimation algorithm. The ASR-UKF has been implemented with the models described in sections III-A and III-B and a real-time comparison between their performance and the conventional methods, namely the simple SoC definition and the Coulomb Counting, has been performed. The Eaton supercapacitor considered for the numerical analysis has been adopted for performing the experimental validation of the SoC estimation methods. As shown in Fig. 4, the supercapacitor has been connected to a Spitzenberger&Spies DM 15000 PAS amplifier used as a bidirectional current source, depending on the imposed current profile. All the SoC estimation methods mentioned in section II, have been implemented in an Opal OP4510 real-time simulator in order to compare their performances with respect to the ideal SoC reference. The SoC estimation task by means of Kalman filtering methods has been set by considering $0.5\ s$ of time step, while the Coulomb Counting and the SoC_{simple}

computations have been executed at $50\ \mu s$ of time step. The diagram of the overall setup is shown in Fig. 5, highlighting the SoC estimation and the measurement tasks performed by the Opal simulator. This also allows for automatically acquiring voltage and current measurements as well as the experimental estimation results. The power amplifier is controlled by a Novacor Real-Time Digital Simulator (RTDS), which elaborates all the necessary signals to perform the tests automatically. In detail, the current profile adopted for characterizing the first model (Fig. 2) has been considered for comparing different SoC estimation methods for Supercapacitors as well. Voltage dividers and current transducers have been adopted to implement a real-world acquisition environment for the estimation algorithms. Fig. 6 shows the results achieved from the experimental test, where each SoC estimation is compared to the reference ideal SoC profile, and the absolute error is considered as a performance indicator. In addition, the temperature of the device under test was monitored during the entire experimental procedure by means of a thermistor placed inside the supercapacitor, which was provided by the EATON manufacturer. A maximum excursion with respect to the ambient temperature lower than 3°C during the overall test has been measured. Therefore, the temperature impact on the estimation results has been considered negligible during the experimental analysis. For what concerns the SoC computation task, the proposed algorithm, which includes the supercapacitor three-branch model, allows for achieving the lowest estimation error during the overall test case, as illustrated in Fig. 6(b). Indeed, a maximum error between 6% and 8% is achieved by the Coulomb Counting and the simple capacity methods, while a noisy result can be noticed in the SoC_{SoA} estimation, mostly due to the voltage measurement noise in the experimental setup. Similarly, the estimation error of the ASR-UKF, integrated with the first-order dynamic equivalent circuit model, reaches a peak value above 6%. On the other hand, if the three-branch model represents the supercapacitor dynamic behavior, despite a slight performance decrease with respect to the numerical results, the proposed estimator ensures an error lower than 2% with respect to the supercapacitor SoC computed in ideal conditions. Therefore, the experimental results validate the performance of the proposed ASR-UKF with the adoption of a three-branch ECM for representing the supercapacitor behavior, which allows for achieving the lowest SoC estimation error among the considered SoC estimators in real-time experimental tests.

VI. Experimental Validation under realistic grid power profiles

Further experimental tests have been performed considering a 1-hour time window extracted from a standard daily power profile measured in a German MV/LV substation [42], which replicates the realistic conditions usually faced when an HESS is adopted. As a plant model, a HESS has been considered, which includes a Supercapacitor module and a Lithium-Ion battery pack, adopting a Low-Pass Filter (LPF) control strategy for allocating the power profiles to the ESS technologies. As a result, the low-frequency variating current has been allocated to the battery, while the supercapacitor has been considered to dampen the current transients and provide the high-frequency power supply required. Moreover, the supercapacitor reference power profile has been scaled down to the EATON supercapacitor voltage and current operating ranges to reproduce in a real-time experimental setup the same scenario experienced in the MV/LV substation. In Fig. 7, the daily power profile is shown, where the 1-hour time window considered in the test is highlighted. The extracted 1-hour power profiles allocated to the battery and the supercapacitor by means of the low-pass filter are depicted in Figs. 7(b) and 7(c), respectively. Figure 7(d) shows the supercapacitor current profile imposed by the power amplifier during the experimental test. It has been obtained by scaling down the power profile to the supercapacitor operating range and dividing the power by the rated voltage of the device. In Fig. 7(e), the SoC computed in ideal conditions and selected as a true reference value, and the SoC estimated by the two conventional methods as well as the estimation performed by the proposed method, are shown. As shown in Fig. 7(f), similar results to the previous tests have been confirmed. The simple capacity model reflects the voltage measurement noise, while the Coulomb Counting method error is included in the $6\% - 8\%$ range. On the other hand, with the proposed ASR-UKF, the error is reduced from the $2\% - 4\%$ range to below 1.5% during the entire test when the three-branch model is considered, thus confirming the better performances in a realistic scenario as well.

VII. Conclusion

This paper proposes a novel method based on the Adaptive Square-Root Unscented Kalman Filter for estimating a supercapacitor's State of Charge. This method was initially developed for batteries and its adaptation to supercapacitors' high variable charging and discharging currents has been discussed in this paper. The three-branch and First-order dynamic electric circuit models have been implemented to represent supercapacitors' behavior and SoC estimation under the new technique. With the help of the Matlab-Simulink® toolbox, an optimal initial calibration of the Kalman filter has been obtained. The SoC estimation for a supercapacitor has been experimentally validated by adopting an EATON 166F supercapacitor. Both Novacor RTDS and Opal OP4510 real-time simulators have been used to control the amplifier and implement the SoC estimation methods, respectively. The results have been compared with the conventional methods, namely the Coulomb Counting and the simple capacitive model, demonstrating the better estimation performance of the proposed method. Further experimental tests under realistic grid power profiles have been performed by considering a 1-hour time window extracted from a German MV/LV substation standard daily power profile. Therefore, the applicability of the estimation algorithm in a Hybrid Energy Storage System has been proven by adopting a classic low-pass filter for power profile allocation. Future developments will be regarding the adoption of advanced power allocation and energy management controllers and the impact of the proposed method on the system performances will be investigated.

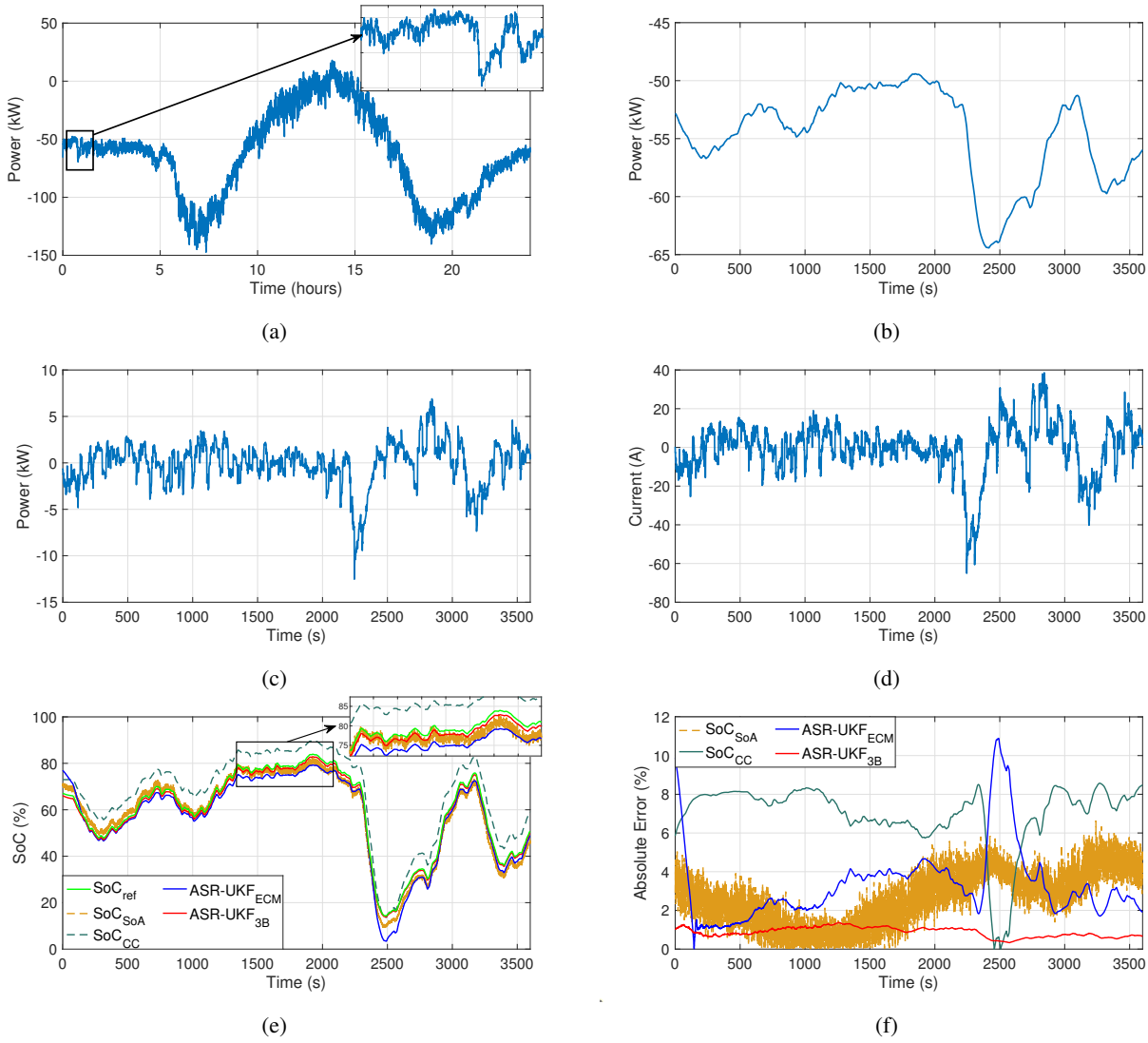

Fig. 7. Experimental results for SoC estimation of supercapacitor in a HESS: (a) daily power reference profile in a German MV/LV substation and considered 1-hour window; (b) power profile allocated to the battery; (c) power profile allocated to the supercapacitor; (d) supercapacitor current profile scaled down to its operating range; (e) SoC estimation results and (f) absolute errors with respect to the ideal SoC reference.

REFERENCES

[1] J. Barton and D. Infield, "Energy storage and its use with intermittent renewable energy," *IEEE Transactions on Energy Conversion*, vol. 19, DOI 10.1109/TEC.2003.822305, no. 2, pp. 441–448, 2004.

[2] X. Li, D. Hui, and X. Lai, "Battery energy storage station (bess)-based smoothing control of photovoltaic (pv) and wind power generation fluctuations," *IEEE Transactions on Sustainable Energy*, vol. 4, DOI 10.1109/TSTE.2013.2247428, no. 2, pp. 464–473, 2013.

[3] F. Nadeem, S. M. S. Hussain, P. K. Tiwari, A. K. Goswami, and T. S. Ustun, "Comparative review of energy storage systems, their roles, and impacts on future power systems," *IEEE Access*, vol. 7, DOI 10.1109/ACCESS.2018.2888497, pp. 4555–4585, 2019.

[4] G. Wang, G. Konstantinou, C. D. Townsend, J. Pou, S. Vazquez, G. D. Demetriades, and V. G. Agelidis, "A review of power electronics for grid connection of utility-scale battery energy storage systems," *IEEE Transactions on Sustainable Energy*, vol. 7, DOI 10.1109/TSTE.2016.2586941, no. 4, pp. 1778–1790, 2016.

[5] S. Hajiaghasi, A. Salemnia, and M. Hamzeh, "Hybrid energy storage system for microgrids applications: A review," *Journal of Energy Storage*, vol. 21, DOI 10.1016/j.est.2018.12.017, pp. 543–570, 2019.

[6] Z. Song, J. Hou, H. F. Hofmann, X. Lin, and J. Sun, "Parameter identification and maximum power estimation of battery/supercapacitor hybrid energy storage system based on cramer–rao bound analysis," *IEEE Transactions on Power Electronics*, vol. 34, DOI 10.1109/TPEL.2018.2859317, no. 5, pp. 4831–4843, 2019.

[7] T. Zimmermann, P. Keil, M. Hofmann, M. F. Horsche, S. Pichlmaier, and A. Jossen, "Review of system topologies for hybrid electrical energy storage systems," *Journal of Energy Storage*, vol. 8, pp. 78–90, 2016.

[8] A. Etxeberria, I. Vechiu, H. Camblong, and J.-M. Vinassa, "Hybrid energy storage systems for renewable energy sources integration in microgrids: A review," in *2010 Conference Proceedings IPEC*, pp. 532–537. IEEE, 2010.

[9] K. W. Wee, S. S. Choi, and D. M. Vilathgamuwa, "Design of a least-cost battery-supercapacitor energy storage system for realizing dispatchable wind power," *IEEE Transactions on Sustainable Energy*, vol. 4, DOI 10.1109/TSTE.2013.2248029, no. 3, pp. 786–796, 2013.

[10] A. Lahyani, P. Venet, A. Guermazi, and A. Troudi, "Battery/supercapacitors combination in uninterruptible power supply (ups)," *IEEE Transactions on Power Electronics*, vol. 28, DOI 10.1109/TPEL.2012.2210736, no. 4, pp. 1509–1522, 2013.

[11] Q. Zhang and G. Li, "Experimental study on a semi-active battery-supercapacitor hybrid energy storage system for electric vehicle application," *IEEE Transactions on Power Electronics*, vol. 35, DOI 10.1109/TPEL.2019.2912425, no. 1, pp. 1014–1021, 2020.

[12] S. Wen, S. Wang, G. Liu, and R. Liu, "Energy management and coordinated control strategy of pv/hess ac microgrid during islanded operation," *IEEE Access*, vol. 7, DOI 10.1109/ACCESS.2018.2887114, pp. 4432–4441, 2019.

[13] S. K. Kollimalla, M. K. Mishra, and N. L. Narasamma, "Design and analysis of novel control strategy for battery and supercapacitor storage system," *IEEE Transactions on Sustainable Energy*, vol. 5, DOI 10.1109/TSTE.2014.2336896, no. 4, pp. 1137–1144, 2014.

[14] B. Wang, C. Wang, Z. Wang, H. Xue, and S. Ni, "Adaptive energy estimation for supercapacitor based on a real-time voltage state observer in electric vehicle applications," *IEEE Transactions on Power Electronics*, vol. 36, DOI 10.1109/TPEL.2020.3044889, no. 7, pp. 7337–7341, 2021.

[15] H. Yang, "Estimation of supercapacitor charge capacity bounds considering charge redistribution," *IEEE Transactions on Power Electronics*, vol. 33, DOI 10.1109/TPEL.2017.2764423, no. 8, pp. 6980–6993, 2018.

[16] A. El Mejdoubi, H. Chaoui, H. Gualous, and J. Sabor, "Online parameter identification for supercapacitor state-of-health diagnosis for vehicular applications," *IEEE Transactions on Power Electronics*, vol. 32, DOI 10.1109/TPEL.2017.2655578, no. 12, pp. 9355–9363, 2017.

[17] R. E. Kalman, "A New Approach to Linear Filtering and Prediction Problems," *Journal of Basic Engineering*, vol. 82, DOI 10.1115/1.3662552, no. 1, pp. 35–45, 03 1960.

[18] G. L. Plett, "Kalman-filter soc estimation for lipb hev cells," 2002.

[19] D. Fusco, M. Di Monaco, F. Porpora, and G. Tomasso, "A novel adaptive square-root unscented kalman filter for battery soc estimation," in *PCIM Europe digital days 2021; International Exhibition and Conference for Power Electronics, Intelligent Motion, Renewable Energy and Energy Management*, pp. 1–8, 2021.

[20] S. Liu, N. Cui, and C. Zhang, "An adaptive square root unscented kalman filter approach for state of charge estimation of lithium-ion batteries," *Energies*, vol. 10, DOI 10.3390/en10091345, no. 9, 2017.

[21] D. Fusco, F. Porpora, M. Di Monaco, V. Nardi, and G. Tomasso, "High performance battery soc estimation method based on an adaptive square-root unscented kalman filter," in *2022 International Symposium on Power Electronics, Electrical Drives, Automation and Motion (SPEEDAM)*, DOI 10.1109/SPEEDAM53979.2022.9842288, pp. 424–429, 2022.

[22] G. De Carne, A. Morandi, and S. Karrari, "Supercapacitor modeling for real-time simulation applications," *IEEE Journal of Emerging and Selected Topics in Industrial Electronics*, vol. 3, DOI 10.1109/JESTIE.2022.3165985, no. 3, pp. 509–518, 2022.

[23] P. Saha, S. Dey, and M. Khanra, "Modeling and state-of-charge estimation of supercapacitor considering leakage effect," *IEEE Transactions on Industrial Electronics*, vol. 67, DOI 10.1109/TIE.2019.2897506, no. 1, pp. 350–357, 2020.

[24] Y. Parvini, J. B. Siegel, A. G. Stefanopoulou, and A. Vahidi, "Supercapacitor electrical and thermal modeling, identification, and validation for a wide range of temperature and power applications," *IEEE Transactions on Industrial Electronics*, vol. 63, DOI 10.1109/TIE.2015.2494868, no. 3, pp. 1574–1585, 2016.

[25] L. Zhang, Z. Wang, H. Xiaosong, and D. Dorrell, "Residual capacity estimation for ultracapacitors in electric vehicles using artificial neural network," 08 2014.

[26] L. Zhang, X. Hu, Z. Wang, F. Sun, and D. G. Dorrell, "A review of supercapacitor modeling, estimation, and applications: A control/management perspective," *Renewable and Sustainable Energy Reviews*, vol. 81, DOI 10.1016/j.rser.2017.05.283, pp. 1868–1878, 2018.

[27] A. Nadeau, M. Hassanalieragh, G. Sharma, and T. Soyata, "Energy awareness for supercapacitors using kalman filter state-of-charge tracking," *Journal of Power Sources*, vol. 296, DOI 10.1016/j.jpowsour.2015.07.050, pp. 383–391, 2015.

[28] M. Ceraolo, G. Lutzemberger, and D. Poli, "State-of-charge evaluation of supercapacitors," *Journal of Energy Storage*, vol. 11, DOI 10.1016/j.est.2017.03.001, pp. 211–218, 2017.

[29] H. Yang, "Estimation of supercapacitor charge capacity bounds considering charge redistribution," *IEEE Transactions on Power Electronics*, vol. 33, DOI 10.1109/TPEL.2017.2764423, no. 8, pp. 6980–6993, 2018.

[30] M. Partovibakhsh and G. Liu, "An adaptive unscented kalman filtering approach for online estimation of model parameters and state-of-charge of lithium-ion batteries for autonomous mobile robots," *IEEE Transactions on Control Systems Technology*, vol. 23, DOI 10.1109/TCST.2014.2317781, no. 1, pp. 357–363, 2015.

[31] X. Hu, S. E. Li, and Y. Yang, "Advanced machine learning approach for lithium-ion battery state estimation in electric vehicles," *IEEE Transactions on Transportation Electrification*, vol. 2, DOI 10.1109/TTE.2015.2512237, no. 2, pp. 140–149, 2016.

[32] J. Wang, L. Zhang, J. Mao, J. Zhou, and D. Xu, "Fractional order equivalent circuit model and soc estimation of supercapacitors for use in hess," *IEEE Access*, vol. 7, DOI 10.1109/ACCESS.2019.2912221, pp. 52 565–52 572, 2019.

[33] S. Dey, S. Mohon, B. Ayalew, H. Arunachalam, and S. Onori, "A novel model-based estimation scheme for battery-double-layer capacitor hybrid energy storage systems," *IEEE Transactions on Control Systems Technology*, vol. 27, DOI 10.1109/TCST.2017.2781650, no. 2, pp. 689–702, 2019.

[34] E. A. Wan and R. Van Der Merwe, "The unscented kalman filter for nonlinear estimation," in *Proceedings of the IEEE 2000 Adaptive Systems for Signal Processing, Communications, and Control Symposium (Cat. No.00EX373)*, DOI 10.1109/ASSPCC.2000.882463, pp. 153–158, 2000.

[35] R. Van der Merwe and E. A. Wan, "The square-root unscented kalman filter for state and parameter-estimation," in *2001 IEEE International Conference on Acoustics, Speech, and Signal Processing. Proceedings (Cat. No.01CH37221)*, vol. 6, DOI 10.1109/ICASSP.2001.940586, pp. 3461–3464 vol.6, 2001.

[36] M. Luzi, M. Paschero, A. Rossini, A. Rizzi, and F. M. F. Mascioli, "Comparison between two nonlinear kalman filters for reliable soc estimation on a prototypal bms," in *IECON 2016 - 42nd Annual Conference of the IEEE Industrial Electronics Society*, DOI 10.1109/IECON.2016.7794054, pp. 5501–5506, 2016.

[37] A. Morandi, A. Lampasi, A. Cocchi, F. Gherdovich, U. Melaccio, P. L. Ribani, C. Rossi, and F. Soavi, "Characterization and model parameters of large commercial supercapacitor cells," *IEEE Access*, vol. 9, DOI 10.1109/ACCESS.2021.3053626, pp. 20 376–20 390, 2021.

[38] L. Zubieta and R. Bonert, "Characterization of double-layer capacitors for power electronics applications," *IEEE Transactions on Industry Applications*, vol. 36, DOI 10.1109/28.821816, no. 1, pp. 199–205, 2000.

[39] V. Sedlakova, J. Sikula, J. Majzner, P. Sedlak, T. Kuparowitz, B. Buergler, and P. Vasina, "Supercapacitor equivalent electrical circuit model based on charges redistribution by diffusion," *Journal of Power Sources*, vol. 286, DOI 10.1016/j.jpowsour.2015.03.122, pp. 58–65, 2015.

[40] J. P. Christophersen, "Battery test manual for electric vehicles, revision 3," DOI 10.2172/1186745, 6 2015.

[41] X. Huang, Y. Li, A. Acharya, X. Sui, J. Meng, R. Teodorescu, and D.-I. Stroe, "A review of pulsed current technique for lithium-ion batteries," *Energies*, vol. 13, DOI 10.3390/en13102458, p. 2458, 05 2020.

[42] S. Karrari, N. Ludwig, G. De Carne, and M. Noe, "Sizing of hybrid energy storage systems using recurring daily patterns," *IEEE Transactions on Smart Grid*, vol. 13, DOI 10.1109/TSG.2022.3156860, no. 4, pp. 3290–3300, 2022.